

# Lawrence Berkeley National Laboratory

## Recent Work

### Title

COLLECTIVE POTENTIAL ENERGY, QUANTUM MECHANICAL FLUCTUATIONS AND TUNNELING EFFECTS IN EVEN NUCLEI I

### Permalink

<https://escholarship.org/uc/item/5323j3x3>

### Author

Kumar, Krishna

### Publication Date

1965-03-01

University of California  
Ernest O. Lawrence  
Radiation Laboratory

COLLECTIVE POTENTIAL ENERGY,  
QUANTUM MECHANICAL FLUCTUATIONS  
AND TUNNELING EFFECTS IN EVEN NUCLEI I

TWO-WEEK LOAN COPY

*This is a Library Circulating Copy  
which may be borrowed for two weeks.  
For a personal retention copy, call  
Tech. Info. Division, Ext. 5545*

## DISCLAIMER

This document was prepared as an account of work sponsored by the United States Government. While this document is believed to contain correct information, neither the United States Government nor any agency thereof, nor the Regents of the University of California, nor any of their employees, makes any warranty, express or implied, or assumes any legal responsibility for the accuracy, completeness, or usefulness of any information, apparatus, product, or process disclosed, or represents that its use would not infringe privately owned rights. Reference herein to any specific commercial product, process, or service by its trade name, trademark, manufacturer, or otherwise, does not necessarily constitute or imply its endorsement, recommendation, or favoring by the United States Government or any agency thereof, or the Regents of the University of California. The views and opinions of authors expressed herein do not necessarily state or reflect those of the United States Government or any agency thereof or the Regents of the University of California.

Research and Development

UCRL-16768  
UC-34 Physics  
TID-4500 (47th Ed.)

UNIVERSITY OF CALIFORNIA  
Lawrence Radiation Laboratory  
Berkeley, California

AEC Contract No. W-7405-eng-48

COLLECTIVE POTENTIAL ENERGY,  
QUANTUM MECHANICAL FLUCTUATIONS  
AND TUNNELING EFFECTS IN EVEN NUCLEI I.

Krishna Kumar

March 1966

Printed in USA. Price \$2.00. Available from the Clearinghouse for Federal  
Scientific and Technical Information, National Bureau of Standards,  
U. S. Department of Commerce, Springfield, Virginia.

COLLECTIVE POTENTIAL ENERGY, QUANTUM MECHANICAL  
FLUCTUATIONS AND TUNNELING EFFECTS IN EVEN NUCLEI I.\*

Krishna Kumar  
Lawrence Radiation Laboratory  
University of California  
Berkeley, California

and

Department of Physics and Astronomy  
Michigan State University  
East Lansing, Michigan+

\* Work performed under the auspices of U.S.A.E.C.

+ Present address.

## Table of Contents

## Abstract

1. Introduction
2. Theoretical Background
  - 2.1 Bohr's Hamiltonian
  - 2.2 Numerical Solutions of Bohr's Hamiltonian
  - 2.3 Quantum Mechanical Fluctuations
  - 2.4 Intrinsic Moments
3. Collective Potential Energy
  - 3.1 Requirements of  $V(\beta, \gamma)$
  - 3.2 Parabolic Expansions of  $V$
  - 3.3 The Myers-Swiatecki Potential
  - 3.4 Extension of the MS Potential
4. Discussion of Results
  - 4.1 Determination of Parameters
  - 4.2 Potential Energy of  $\text{Sm}^{154}$
  - 4.3 Comparison with the Rotational Model
  - 4.4 Detailed Study of Effects of  $V$
5. Summary and Conclusions

Acknowledgments

References

Table Captions

Tables

Figure Captions

Figures

COLLECTIVE POTENTIAL ENERGY, QUANTUM MECHANICAL  
FLUCTUATIONS AND TUNNELING EFFECTS IN EVEN NUCLEI I.

Krishna Kumar

Lawrence Radiation Laboratory  
University of California  
Berkeley, California

and

Department of Physics and Astronomy  
Michigan State University  
East Lansing, Michigan

March 1966

## Abstract

A dynamical description of collective quadrupole motion is given. Quantum mechanical fluctuations of nuclear shapes and their effects on coupling between rotations and vibrations, and between  $\beta$ -vibrations and  $\gamma$ -vibrations are investigated. These effects indicate the need of a more complicated  $\beta$ -,  $\gamma$ -dependence of the collective potential energy than that used in the past. A potential function, which is an extension of the Myers-Swiatecki potential, is suggested. On using this extended potential, good agreement is obtained with the experimental energy levels and  $B(E2)$  values of  $\text{Sm}^{154}$ . The general nature of the potential is utilized to gain some qualitative understanding of other nuclei. A metastable band, which represents quantum mechanical tunneling and which can decay to the ground band only through a cascade involving one of the excited bands, is predicted.



## 1. Introduction

The Bohr-Mottelson<sup>1,2</sup> description of collective quadrupole motion, approximated by a vibrational model in case of spherical nuclei and by a rotational model in case of deformed nuclei, has been widely used for understanding low energy properties of nuclei<sup>3</sup>. The energy levels and transition probabilities of nuclei often deviate from the predictions of these idealized models. For example, the two phonon triplet of spherical nuclei is usually split<sup>4</sup> and the excitation energies of deformed nuclei often deviate from the  $I(I+1)$  rule<sup>5</sup>. The purpose of the present investigation, of which this is a preliminary report, is to understand these deviations, as well as the basic assumptions of the vibrational and rotational models, by giving a dynamic description of nuclear deformations.

Baranger and Kumar<sup>6,7</sup> have recently developed an exact, numerical method of calculating energy levels, static moments, and transition probabilities corresponding to a given Bohr's collective Hamiltonian<sup>1</sup>. This method makes the adiabatic approximation that the intrinsic motion follows the collective motion of a nucleus. However, the shape and hence the intrinsic motion of the nucleus is free to change from one nuclear state to another one. In fact, the collective wavefunction of each stationary state is in general a linear combination of many different intrinsic wavefunctions. Therefore, this dynamical adiabatic approximation is an improvement over the approximation where the shape of a nucleus is considered to be static or capable of executing only harmonic vibrations. This method does not make the usual assumptions

about (a) the separation of rotations and vibrations or (b) the separation of  $\beta$ - and  $\gamma$ -motions. Thus, it is possible to test these assumptions. Of particular interest are quantum mechanical fluctuations in the shape of a nucleus which can be different for different states of the same nucleus.

In the numerical method mentioned above, the kinetic energy and potential energy of Bohr's Hamiltonian can be any arbitrary functions of nuclear deformations, subject only to the symmetry requirements of the Hamiltonian. In the present paper, the kinetic energy of deformation has the Bohr form<sup>1</sup> which can be expressed in terms of a single inertial parameter. However, the potential energy of deformation,  $V(\beta, \gamma)$ , is given special consideration.

In most of the analytic or perturbative methods<sup>8,9</sup> of solving Bohr's Hamiltonian, the potential energy is a quadratic function of deformation. The equilibrium point occurs either for a spherical shape or for a deformed shape. However, with the probability of large fluctuations in the deformation, the assumption of quadratic potential energy cannot be expected to be good, one reason among many being that, with a deformed equilibrium shape, it does not satisfy the proper symmetry requirements of Bohr's Hamiltonian.

Myers and Swiatecki<sup>10</sup> have recently suggested a semi-empirical formula for  $V(\beta, \gamma)$ . They obtain the values of the constants of this function by fitting the ground state binding energies and quadrupole moments, and fission barriers of all nuclei. This potential function has several remarkable features. (1) It does not require a priori knowledge of the shape of a nucleus.

The lowest minimum of the potential determines whether the nucleus under consideration is spherical or deformed. (2) It satisfies the symmetry requirements of Bohr's Hamiltonian. (3) Additional terms can be included without affecting the nuclear behaviour at large deformations which lead to fission.

In this paper, we take the MS (Myers-Swiatecki) potential as our starting point and search for the potential energy of a well-deformed nucleus like  $\text{Sm}^{154}$ . Then, we study the effects of various terms of  $V(\beta, \gamma)$  on the energy levels. We try to answer some of the usual questions. What terms of  $V$  are responsible for anharmonicity or deviations from a pure phonon spectrum? What is the role played by prolate-oblate differences? What are the effects of lack of axial symmetry? What are the effects of coupling between (a) rotations and vibrations, and (b) the  $\beta$ - and  $\gamma$ - motions of a nucleus? How big are the quantum mechanical fluctuations and how do they depend on nuclear states?

Quantitative results are given for  $\text{Sm}^{154}$ . The general nature of the method is then utilized to make some qualitative conclusions about other deformed nuclei.

## 2. Theoretical Background

### 2.1 Bohr's Hamiltonian

A phenomenological treatment of quadrupole deformations is provided by Bohr's collective Hamiltonian<sup>1</sup>. This is a classical Hamiltonian involving five coordinates describing both the orientation and the shape of the quadrupole. The orientation is specified by Euler angles  $\theta, \phi, \psi$ , while the shape is determined

by two variables,  $\beta$  and  $\gamma$ . The three intrinsic radii  $R_1, R_2, R_3$  are given in terms of  $\beta$  and  $\gamma$  by

$$R_1 = R_0 \left[ 1 + \left( \frac{5}{4\pi} \right)^{1/2} \beta \cos (\gamma - 120^\circ) \right], \quad (1a)$$

$$R_2 = R_0 \left[ 1 + \left( \frac{5}{4\pi} \right)^{1/2} \beta \cos (\gamma + 120^\circ) \right], \quad (1b)$$

$$R_3 = R_0 \left[ 1 + \left( \frac{5}{4\pi} \right)^{1/2} \beta \cos \gamma \right], \quad (1c)$$

$R_0$  being the average radius of the nucleus.

Then, Bohr's Hamiltonian is

$$H = V(\beta, \gamma) + T_{rot} + T_{vib}. \quad (2)$$

The first term is the potential energy of deformation and will be discussed in Sec. 3. The second is the rotational kinetic energy

$$T_{rot} = \frac{1}{2} \left[ \mathcal{I}_1(\beta, \gamma) \omega_1^2 + \mathcal{I}_2(\beta, \gamma) \omega_2^2 + \mathcal{I}_3(\beta, \gamma) \omega_3^2 \right], \quad (3)$$

where  $I_1, I_2, I_3$  are the three principal moments of inertia, and  $\omega_1, \omega_2, \omega_3$  are the components of the angular velocity on the intrinsic axes. The third term of  $H$  is the vibrational kinetic energy

$$T_{vib} = \frac{1}{2} B_{\beta\beta}(\beta, \gamma) \dot{\beta}^2 + B_{\beta\gamma}(\beta, \gamma) \dot{\beta} \dot{\gamma} + \frac{1}{2} B_{\gamma\gamma}(\beta, \gamma) \dot{\gamma}^2. \quad (4)$$

In Bohr's formulation, the six inertial coefficients,  $I$ 's and  $B$ 's, have the forms

$$I_k(\beta, \gamma) = 4 B \beta^2 \sin^2 \left( \gamma - \frac{2\pi}{3} k \right), \quad (k=1, 2, 3) \quad (5)$$

$$B_{\beta\beta} = B, \quad B_{\beta\gamma} = 0, \quad B_{\gamma\gamma} = \beta^2 B. \quad (6)$$

Thus, the total kinetic energy depends on a single inertial parameter,  $B$ . Even though the numerical method used (Sec. 2.2) can handle any arbitrary forms of the six inertial coefficients, we use Bohr's form because of the obvious simplification and low number of parameters. In fact, we have done some experimentation by using a different  $B$  for  $\gamma$ -vibrations<sup>11</sup>, as compared to the  $B$  for  $\beta$ -vibrations and rotations. However, it does not lead to any

significant improvement of the results of Sm<sup>154</sup>.

## 2.2 Numerical Solutions of Bohr's Hamiltonian

Collective energy  $E_{\lambda I}$  and wavefunction  $\Psi_{\lambda I M}$  corresponding to a stationary state with angular momentum  $I$ ,  $Z$ -component  $M$ , and other quantum numbers  $\lambda$ , are determined by solving the equation

$$H \Psi_{\lambda I M} = E_{\lambda I} \Psi_{\lambda I M} \quad (7)$$

where  $H$  is Bohr's Hamiltonian. The wavefunction is written as<sup>1,6,7</sup>

$$\Psi_{\lambda I M}(\beta, \gamma, \theta, \phi, \psi) = \sum_K A_{\lambda I K}(\beta, \gamma) \Psi_{I M K}(\theta, \phi, \psi) \chi(\beta, \gamma), \quad (8a)$$

$$\Psi_{I M K}(\theta, \phi, \psi) = \left[ \frac{(2I+1)}{16\pi^2(1+\delta_{K0})} \right]^{\frac{1}{2}} \left[ \mathcal{D}_{MK}^I(\theta, \phi, \psi) + (-)^I \mathcal{D}_{M, -K}^I(\theta, \phi, \psi) \right], \quad (8b)$$

where  $\chi$  is the intrinsic wavefunction of the nucleus,

$K$  is the projection of  $I$  on the  $k=3$  axis of the intrinsic system

and takes even, positive values only [ $K=0, 2, \dots, I$  for even  $I$ ;

$K=2, 4, \dots, (I-1)$  for odd  $I$ ], and  $\mathcal{D}$ 's are the usual rotational

matrices<sup>12</sup>. There is a summation over  $K$  in Eq. (8a) since

rotation-vibration interaction can lead to band mixing and then

$K$  is not a good quantum number. Also, the usual separation of

the wavefunction  $A_{\lambda IK}(\beta, \gamma)$  into a  $\beta$ -dependent part and a  $\gamma$ -dependent part is not made since these two motions are in general not independent.

The wavefunctions  $A_{\lambda IK}(\beta, \gamma)$  are computed by using KATIE, a Fortran code written by the author. This code employs the numerical method developed by Baranger and Kumar<sup>6,7</sup> and the details are given in the references cited. Examples of wavefunctions calculated by using KATIE are shown in Figures 4-7. In these plots,  $\beta$  is the radial coordinate, and  $\gamma$  is the angular coordinate which varies from  $0^\circ$  to  $60^\circ$ . It can be seen from Eqs. (1) that it is sufficient to vary  $\gamma$  from  $0^\circ$  to  $60^\circ$ . The  $\beta$ - $\gamma$  region consists of a large equilateral triangle which is divided into 256 small triangles. Values of  $A_{\lambda IK}$  are computed at all the points of this  $\beta$ - $\gamma$  mesh. The left hand corner of the large triangle corresponds to  $\beta=0$ , while the right hand corner and the uppermost corner correspond to  $\beta = \beta_m$ . Value of  $\beta_m$  or the cutoff point for numerical integrations is determined by testing the convergence of the numerical solutions and is 0.65 for the  $Sm^{154}$  wavefunctions shown in Figures 4-7. The method of calculation of these wavefunctions will be discussed later. They are normalized in accordance with the relation<sup>1</sup>

$$1 = 2B^{5/2} \sum_K \int_0^\infty d\beta \beta^4 \int_0^{\pi/3} d\gamma \sin 3\gamma A_{\lambda IK}^2(\beta, \gamma). \quad (9)$$

### 2.3 Quantum Mechanical Fluctuations

Keeping the symmetry properties in mind, we define

$$f_0 = \langle I | \beta^2 \cos^2 3\gamma | I \rangle - \langle I | \beta \cos 3\gamma | I \rangle^2, \quad (10)$$

$$f_2 = \langle I | \beta^2 \sin^2 3\gamma | I \rangle - \langle I | \beta \sin 3\gamma | I \rangle^2, \quad (11)$$

$$f = \langle I | \beta^2 | I \rangle - \langle I | \beta \cos 3\gamma | I \rangle^2 - \langle I | \beta \sin 3\gamma | I \rangle^2 \quad (12)$$

$$= f_0 + f_2, \quad (13)$$

$$\beta_{r.m.s.} = \langle I | \beta^2 | I \rangle^{\frac{1}{2}}, \quad (14)$$

$$\gamma_{r.m.s.} = \frac{1}{3} \tan^{-1} \left[ \frac{\langle I | \beta^2 \sin^2 3\gamma | I \rangle}{\langle I | \beta^2 \cos^2 3\gamma | I \rangle} \right]^{\frac{1}{2}}, \quad (15)$$

where  $I$  denotes a stationary, nuclear state (Eqs. 8), and  $\beta_{r.m.s.}$ ,  $\gamma_{r.m.s.}$  refer to root mean square values. Using the relations



$$\beta \cos 3(-\gamma) = \beta \cos 3\gamma, \quad \beta \cos 3(\gamma-120^\circ) = \beta \cos 3\gamma, \quad (16)$$

$$\beta \sin 3(-\gamma) = -\beta \sin 3\gamma, \quad \beta \sin 3(\gamma-120^\circ) = \beta \sin 3\gamma, \quad (17)$$

the integrals over  $\gamma=0^\circ$  to  $360^\circ$  can be easily reduced to integrals over  $\gamma=0^\circ$  to  $60^\circ$  only. In fact, the integral  $\langle I | \beta \sin 3\gamma | I \rangle$  is always zero, but  $\langle I | \beta \cos 3\gamma | I \rangle$  vanishes only if the wavefunction is symmetric around  $\gamma=30^\circ$ . We also calculate the separation parameter  $\mu$ , defined by Davydov<sup>13</sup>, which is written in our notation as

$$\mu = (2f)^{\frac{1}{2}} / \beta_{\text{r.m.s.}} \quad (18)$$

#### 2.4 Intrinsic Moments

Expectation values of the quadrupole operators for an intrinsic state  $|\chi(\beta, \gamma)\rangle$ , obtained by assuming uniform charge distribution and using Bohr's definitions (Eqs. 1), are found to be

$$\begin{aligned} Q_0 &= \langle \chi | (16\pi/5)^{\frac{1}{2}} r^2 Y_{20} | \chi \rangle \\ &= [3/(5\pi)^{\frac{1}{2}}] Z R_0^2 \beta [\cos \gamma + (5/64\pi)^{\frac{1}{2}} \beta \cos 2\gamma], \quad (19a) \end{aligned}$$

$$Q_2 = \langle \chi | (8\pi/5)^{\frac{1}{2}} \mathcal{R}^2 (Y_{2,2} + Y_{2,-2}) | \chi \rangle$$

$$= [3/(5\pi)^{\frac{1}{2}}] Z R_0^2 \beta \sin \gamma [1 - (5/16\pi)^{\frac{1}{2}} \beta \cos \gamma], \quad (19b)$$

where  $R_0$  is the average nuclear radius given by

$$R_0 = 1.2 A^{1/3} \times 10^{-13} \text{ cm.} \quad (20)$$

Note that the expectation values of  $M=\pm 1$  components of the quadrupole operator vanish and those of  $M=\pm 2$  components are equal in the intrinsic system. When  $\gamma=0^\circ$ ,  $Q_2=0$  and Eq. (19a) reduces to the familiar form<sup>8</sup>.

### 3. Collective Potential Energy

#### 3.1 Requirements of $V(\beta, \gamma)$

(a) The Collective Hamiltonian and hence the potential function,  $V(\beta, \gamma)$ , must satisfy the invariance requirements discussed by Bohr<sup>1</sup>. In particular, the nuclear shape and the corresponding potential energy must be independent of the choice of the axes. It can be seen from Eqs. (1) that the transformations  $(\beta, \gamma) \rightarrow (\beta, -\gamma)$  and  $(\beta, \gamma) \rightarrow (\beta, \gamma - 120^\circ)$  correspond to a simple relabelling of the three axes and hence represent the same nuclear shape. Therefore, we must have

$$V(\beta, \gamma) = V(\beta, -\gamma) = V(\beta, \gamma - 120^\circ). \quad (21)$$

Hence the only terms that can be used in an expansion of  $V(\beta, \gamma)$  are  $\beta \cos 3\gamma$ ,  $\beta^2$ , or some combinations of these two invariants.

- (b) It can be shown from very general considerations, for example the self-consistency requirements<sup>14</sup> of a Hartree-Fock type of calculation, that the spherical shape ( $\beta=0$ ) should always be a solution<sup>15</sup> of the Hamiltonian. Hence,  $V$  must satisfy the condition

$$\partial V / \partial \beta = 0 \quad \text{at} \quad \beta = 0. \quad (22)$$

In other words,  $V$  should not have any linear terms in  $\beta$ . Similar conditions on the  $\gamma$ -dependence require that

$$\partial V / \partial \gamma = 0 \quad \text{at} \quad \gamma = n\pi/3. \quad (n=0, 1, 2, \dots) \quad (23)$$

Combining these conditions with those discussed before, we find that the lowest order allowable terms are  $\beta^2$ ,  $\beta^2 \cos^2 3\gamma$ ,  $\beta^2 \sin^2 3\gamma$ ,  $\beta^3 \cos 3\gamma$ , etc.

- (c) According to a Wilets-Jean<sup>16</sup> theorem, any  $\gamma$ -independent potential leads to degeneracy of the first excited 4+ state and the second excited 2+ state. In the rotational nuclei, the former state belongs to the ground band and the latter to either a  $\beta$ -vibrational band or a  $\gamma$ -vibrational band. In the vibrational model, the two states belong to the two phonon triplet. The two states are usually non-degenerate in actual nuclei. Therefore, it is essential that the potential function must have an adequate  $\gamma$ -dependence.<sup>17</sup>
- (d) The potential function should be suitable for spherical, as well as deformed nuclei since it would be desirable to have a unified picture for both kinds of nuclei. This might also enable us to study transitions from one kind of nuclei to another kind.

### 3.2 Parabolic Expansions of V

The usual parabolic expansion of V around a deformed shape<sup>8,9</sup>

$$V(\beta, \gamma) = \frac{1}{2} C_{\beta} (\beta - \beta_0)^2 + \frac{1}{2} C_{\gamma} (\gamma - \gamma_0)^2, \quad (\beta_0 \neq 0) \quad (24)$$

has been a useful guide in our understanding of  $\beta$ - and  $\gamma$ -vibrations. However, such a potential does not satisfy the requirements discussed in Sec. 3.1. Eq. (24) yields different potential values

for the same nuclear shape depending upon how the intrinsic axes are labelled. Also, this potential does not have the correct behavior at  $\beta=0$  or at  $\gamma = n\pi/3$  ( $C_\gamma \neq 0$ ).

The parabolic expansion of  $V$  around a spherical shape<sup>1</sup>,  $v = \frac{1}{2} C \beta^2$  does satisfy the requirements (a) and (b) of Sec. 3.1. However, it leads to a pure vibrational spectrum with a degenerate, two phonon triplet. Additional terms are needed to obtain the spectrum of a realistic nucleus.

### 3.3 The Myers-Swiatecki Potential

From their considerations of binding energies, quadrupole moments, and fission barriers of all nuclei, Myers and Swiatecki obtain<sup>10</sup>

$$V(\beta, \gamma) = \frac{1}{2} C \beta^2 - f \beta^3 \cos 3\gamma + G_0 \exp(-\beta^2/a^2). \quad (25)$$

They give extensive tables of the values of  $C$ ,  $f$ ,  $G_0$ , and  $a$ . These values vary fairly regularly over the nuclear chart. The first two terms of Eq. (25) correspond to changes in the surface energy and the Coulomb energy of deformation of a liquid drop nucleus. The  $f$ -term leads to fission at large deformations. The third term of Eq. (25) is attributed to shell effects<sup>10</sup>, the fact that the single particle shell model levels are not uniformly spaced.

These shell effects disappear at large deformations and do not affect nuclear fission. In case of nuclei near closed shells,  $G_0 < 0$  and the nuclei are even more tightly bound than the  $\frac{1}{2} C \beta^2$  term would suggest. In case of nuclei away from closed shells,  $G_0 > 0$  and the lowest potential minimum corresponds to a deformed shape.

The MS potential has several remarkable features which have been listed in Sec. 1. However, as we shall see later, it is not enough. Since the  $f$ -term is usually small, this potential is practically  $\gamma$ -independent and the  $2^+$  state and the  $4^+$  state of a nucleus are almost degenerate. Therefore, additional terms are needed.

### 3.4 Extension of the MS Potential

Keeping the requirements of the potential, discussed in Section 3.1, in mind, a search is made for additional terms of the potential function. The calculated energy levels and  $B(E2)$ 's are compared with the experimental data of  $\text{Sm}^{154}$ . We find it necessary to add two  $\gamma$ -dependent terms to the MS potential and write the resulting potential function as

$$V(\beta, \gamma) = \frac{1}{2} C \beta^2 - f \beta^3 \cos 3\gamma + [G_0 + G_1 (\beta^3/a^3) \cos 3\gamma + G_2 (\beta^2/a^2) \sin^2 3\gamma] \exp(-\beta^2/a^2). \quad (26)$$

Both the  $G_1$ - and  $G_2$ - Gaussians vanish at large deformations and hence do not affect nuclear fission. The  $G_1$ -term affects

the relative positions of the prolate ( $\gamma=0^\circ$ ) and oblate ( $\gamma=60^\circ$ ) minima of  $V$ . When  $G_1$  is negative, the prolate minimum is lowered. The reverse happens for positive values of  $G_1$ . The  $G_2$ -term does not affect the axially symmetric part ( $\gamma=0^\circ$  or  $60^\circ$ ) of  $V$ , but creates a hill ( $G_2 > 0$ ) or valley ( $G_2 < 0$ ) at  $\gamma=30^\circ$ . Effects of these terms on the collective properties are discussed in Sec. 4.

#### 4. Discussion of Results

##### 4.1 Determination of Parameters

The collective properties that are discussed in this paper involve essentially low energies and small deformations as compared to the fission barrier of a nucleus. Therefore, we have nothing new to say about the first two terms of Eq. (26). The coefficients  $C$  and  $f$  are taken from the MS tables and are considered to be fixed. However, we do need to modify the shell function of the MS potential in order to get a reasonable agreement with the experimental data. Therefore, we treat the Gaussian coefficients  $G_0$ ,  $G_1$ , and  $G_2$  of Eq. (26) as adjustable parameters and determine them by fitting the known experimental data. The Gaussian range,  $\alpha$ , is treated as a fixed parameter since its main effect is to determine the magnitude of nuclear deformation and hence small changes in  $\alpha$  do not change the nature of the nuclear spectrum. We use a value of  $\alpha=0.3$  for  $\text{Sm}^{154}$ . Our estimate is considerably larger than that used by MS, but it is probably more realistic because (1) the magnitude of experimental deformation is about  $\alpha=0.3$  in the region considered and (2) a look at Nilsson levels<sup>18</sup> reveals that the shell effects do not disappear until after  $\beta \gg 0.3$ .

We have an additional parameter, namely the inertial parameter  $B$  of the kinetic energy (Eqs. 3 to 6). An estimate of  $B$  can be obtained as follows. Grodzins<sup>19</sup> has given a semi-empirical relation for the transition probability

$$T(E2; 2 \rightarrow 0) = 3 \times 10^{10} (E \text{ in Mev})^4 \left( \frac{Z^2}{A} \right) \text{ sec.}^{-1}, \quad (27)$$

where  $E$  is the excitation energy of the first  $2+$  state. Combining this relation with the rotational model<sup>2</sup>, one obtains (using the notation where  $\hbar = c = 1$ )

$$B = 10^{-3} \times A^{7/3} \text{ Mev}^{-1}. \quad (28)$$

This gives a value of  $B = 127 \text{ (Mev)}^{-1}$  for  $\text{Sm}^{154}$  and the same has been used in our calculations.

#### 4.2 Potential Energy of $\text{Sm}^{154}$

A comparison of the calculated energy levels and  $B(E2)$ 's with the experimental data<sup>20</sup> is shown in Fig. 1. Good agreement is obtained. The collective potential energy used for these results is shown in Fig. 2. Effects of various terms of  $V$  on the energy levels of  $\text{Sm}^{154}$  are shown in Fig. 3. The column (a) corresponds to the first term of Eq. (26) which leads to the well-known



phonon spectrum with a two phonon triplet of  $0^+, 2^+, 4^+$ . Column (b) of Fig. 3 corresponds to the first two terms of Eq. (26). Comparison with column (a) shows that the effect of the  $f \beta^3 \cos 3\gamma$  term is negligible at this stage. Hence, this term is not the main cause of anharmonicity. It should be noted here that (1) the ' $f$ ' term could not be made arbitrarily large otherwise the nucleus would fission at unusually low energies and deformations, and (2) additional terms in the expansion of  $V$  become important near the fission barrier<sup>10</sup> but are unimportant for our purposes.

Column (c) of Fig. (3) corresponds to the first three terms of Eq. (26). This is the MS potential except for the different magnitude and range of the Gaussian. This  $G_0$ -Gaussian lowers all the energy levels dramatically. The lowest three levels have the rotational sequence  $0^+, 2^+, 4^+$ . Also, there is a dramatic change in the value of  $B(E2, 0 \rightarrow 2)$  from 1.0 to 3.7 (not shown in the figure) which indicates that the nucleus has deformed. However, similarity with the rotational picture ends there. The energy levels of a rotational nucleus are characterized by an energy gap of about 1 Mev between the  $4^+$  state of the ground band and the  $2^+$  state which should belong to a  $\beta$ -band or a  $\gamma$ -band. (See, for example, the experimental spectrum shown at the right of the figure.) Instead, in case of the spectrum shown in column (c), the  $4^+$  and  $2^+$  states are almost degenerate. The reason is that the MS potential is practically  $\gamma$ -independent since the  $f$ -term is small. Therefore, there is quantum mechanical tunneling between the prolate and oblate minima of the potential

at rather low energies. Interaction between rotation and vibration is strong and  $K$  is not a good quantum number at all.

Column (d) corresponds to the first four terms of  $V$  (Eq. 26). Comparison with column (c) shows that the  $G_1$ -Gaussian, which has a negative value in this case and lowers the prolate minimum as compared to the oblate one, does create an appropriate gap of the kind mentioned above. However, the  $\beta$ -band and the  $\gamma$ -band are almost degenerate -- in fact, the  $\gamma$ -band is lower -- in contradiction with the experimental data.

Column (e) shows the effect of adding the  $G_2$ -Gaussian to the potential of column (c). This term separates the prolate and oblate minima by creating a hill at  $\gamma=30^\circ$ . This has the effect of creating an oblate band with its bandhead  $0^+$  at an excitation energy of 0.6 Mev only. It is perhaps not impossible that both prolate and oblate bands may exist at fairly low energies in some nuclei. But this does not seem likely in case of  $\text{Sm}^{154}$ . Therefore, we conclude that it is essential to have a term of the type discussed in the previous paragraph which creates a substantial prolate-oblate difference. The  $G_2$ -Gaussian also plays an essential role in that it removes the near degeneracy of the  $\beta$ -band and the  $\gamma$ -band of col. (d). The resulting spectrum is shown in col. (f) which is in rather good agreement with the experiment. Since these calculations require about 10 minutes of CDC3600 for each run, most of our calculations are done for only the nuclear states shown in Fig. 3. Some additional states are also calculated and are shown in Fig. 1.

Some of the collective wavefunctions,  $A_{IK}$ , for  $\text{Sm}^{154}$  are shown in Figs. 4 to 7.

### 4.3 Comparison with the Rotational Model

Here, our purpose is to understand some basic assumptions of the rotational model<sup>1,2</sup>. For a given Hamiltonian, many quantities can be calculated by using the standard techniques. For example, the excitation energies of the ground band of a prolate nucleus ( $\bar{\gamma} = 0^\circ$ ) are given by

$$E_{\mathbb{I}} = \mathbb{I}(\mathbb{I}+1)/2 \mathcal{A} \quad , \quad (29)$$

where

$$\mathcal{A} = \mathcal{A}_1(\bar{\beta}, \bar{\gamma} = 0^\circ) = \mathcal{A}_2(\bar{\beta}, \bar{\gamma} = 0^\circ) = 3B\bar{\beta}^2 \quad , \quad (30)$$

and  $\bar{\beta}, \bar{\gamma}$  refer to the lowest minimum of  $V(\beta, \gamma)$ . Energies of the  $\beta$ -phonon ( $E_{0'+}$ ) and the  $\gamma$ -phonon ( $E_{2''+}$ ) are given by

$$E_{0'+} = \left[ (\partial^2 V / \partial \beta^2) / B \right]^{1/2} \quad , \quad (31)$$

$$E_{2''+} = \left[ (\partial^2 V / \partial \gamma^2) / B \bar{\beta}^2 \right]^{1/2} \quad . \quad (32)$$

The  $B(E2)$  value connecting the lowest two states of the ground band is given by

$$B(E2; 0 \rightarrow 2) = (5/16\pi) Q_0^2, \quad (33)$$

where  $Q_0$  is the intrinsic quadrupole moment, defined by Eq. (19a), and calculated at  $\beta = \bar{\beta}$ ,  $\gamma = \bar{\gamma} = 0^\circ$ . Branching ratios for the intra-band transitions are given by<sup>15</sup> the ratios of Clebsch-Gordan coefficients:

$$\frac{B(E2; I_i K_i \rightarrow I_f K_f)}{B(E2; I_i' K_i' \rightarrow I_f' K_f')} = \frac{\left( \begin{matrix} I_i & 2 & I_f \\ K_i & K & K_f \end{matrix} \right)^2}{\left( \begin{matrix} I_i' & 2 & I_f' \\ K_i' & K' & K_f' \end{matrix} \right)^2}. \quad (34)$$

The spectroscopic quadrupole moment of a state  $I, K$  is given by<sup>2</sup>

$$Q_I = \left[ \frac{3K^2 - I(I+1)}{I(I+1)(2I+3)} \right] Q_0. \quad (35)$$

Values calculated according to the above formulae are compared with the results of the dynamic method used in the present paper and are given in Table 1. Agreement in the results of the two methods of calculation is rather good. The main effects of the

dynamics are the following. Energy of the first excited state is increased by 15%, or the effective moment of inertia is decreased by 10%. Energy of the  $\beta$ -phonon is decreased by 15% and that of the  $\gamma$ -phonon by 20%. The branching ratio involving decay of the  $2^+$  state of the  $\beta$ -band is reduced by a factor of 2.

The main reason for the good agreement seems to be that  $K$  is a rather good quantum number for the bands discussed above. This implies that coupling between rotations and vibrations is not significant in this nucleus. The disagreements are probably due to coupling between the  $\beta$ -motion and the  $\gamma$ -motion of the nucleus. This coupling is caused by quantum mechanical fluctuations in the shape of the nucleus. Magnitudes of these fluctuations and root mean square values of the deformation variables  $\beta$  and  $\gamma$  are given in Table 2. As the excitation energy is increased, the root mean square values do not change significantly but the fluctuations become larger. Also, the separation parameter  $\mu$  (Eq. 18) becomes larger. Our calculated values of  $\mu$  are always much larger than the upper limit of  $1/3$  suggested by Davydov<sup>13</sup> as a criterion for the separation of  $\beta$ -motion and  $\gamma$ -motion.

Large fluctuations at high excitation energies lead to quantum mechanical tunneling between the prolate and the oblate minima of the potential and create a metastable band, denoted by  $m$ -band. The present theory predicts the head of this band to be a  $0^+$  state at an excitation energy of 1.879 Mev (Fig. 1). This band is metastable in the sense that direct  $E2$  transitions from the states of this band to those of the ground band are highly forbidden. It can be seen from Fig. 1 that the most probable mode of decay of this band is through the cascade  $4^+ \rightarrow 2^+ \rightarrow 0^+ \rightarrow 2^+ \rightarrow 0^+ \rightarrow 2^+ \rightarrow 0^+$

involving states of the  $\beta$ -band.

#### 4.4 Detailed Study of Effects of V

In this subsection, we present results of variation of the three Gaussian terms of Eq. (26). Other parameters are the same as those used for our  $\text{Sm}^{154}$  calculation. The results are shown in Figs. 8-10. Fig. 8 shows the effects of the  $G_0$ -term ( $G_1=G_2=0$ ). For  $G_0=0$ , we have a spherical nucleus with the usual phonon spectrum. As  $G_0$  is given increasingly negative values, the nucleus becomes more tightly bound. Its collective wavefunction is more highly concentrated around  $\beta=0$  and hence the  $B(E2)$  value decreases. The two phonon triplet is split, but the  $2^+$  and  $4^+$  states remain degenerate because of  $\gamma$ -independence of the potential. When  $G_0$  is made positive, there is a general collapse of the phonon spectrum and the  $B(E2)$  value increases sharply. The nucleus gets deformed but there is too much coupling between the various motions.

Effects of the  $G_1$ -term ( $G_0=10 \text{ Mev}, G_2=0$ ) are shown in Fig. 9. Negative values of  $G_1$  lower the prolate minimum relative to the oblate one. Positive values of  $G_1$  have the opposite effect. Spectra on the two sides of the  $G_1=0$  column are almost the same except for the slight difference due to the  $f$ -term of the MS potential which favors prolate over oblate. Thus, one cannot distinguish between prolate and oblate deformations on the basis of energy levels alone. One has to determine the signs of quadrupole moments of excited states.

Effects of the  $G_2$ -Gaussian ( $G_0=10 \text{ Mev}, G_1=0$ ) are shown in Fig. 10. Positive values of  $G_2$  create a hill at  $\gamma=30^\circ$  and hence increase the tendency towards axial symmetry. The band starting at  $0^+$

state is not the usual  $\beta$ -vibrational band, but is an oblate band since the corresponding wavefunction (not shown in the fig.) is concentrated around the  $\gamma=60^\circ$  axis. Negative values of  $G_2$  create a valley at  $\gamma=30^\circ$  and the nucleus becomes asymmetric or "non-axial", and a Davydov-Filippov<sup>21</sup> type of spectrum is obtained. The prediction made by Das-Gupta and Gunye<sup>23</sup> about the lowering of  $2^+$  state below  $4^+$  is confirmed. However, the  $\beta$ -band is pushed to very high excitation energies.

It is hoped that these figures will be useful in learning about the  $\gamma$ -dependence of the potential of a nucleus. However, it should be kept in mind that each term of the potential affects all the energy levels and wavefunctions and therefore only qualitative conclusions can be drawn without doing the actual calculation for a particular nucleus. Also, it is necessary to have reliable data about both the  $\beta$ -band and the  $\gamma$ -band of a nucleus before one can arrive at any meaningful conclusions.

## 5. Summary and Conclusions

The  $\beta$ - $\gamma$ -dependence of collective potential energy of a well-deformed nucleus like  $\text{Sm}^{154}$  is investigated by using a numerical method of solving Bohr's Hamiltonian. The potential function of Myers and Swiatecki is used as a starting point. Two  $\gamma$ -dependent Gaussians are added to their potential. One of them increases the prolate-oblate difference, while the other term separates the two minima by creating a hill or a valley at  $\gamma=30^\circ$ . The former term is essential for preventing quantum mechanical tunneling at unrealistically low energies and thus providing an energy gap between the ground band and the excited bands. The later term is needed to

separate the  $\beta$ -band and the  $\gamma$ -band of the nucleus.

While the coupling between low energy rotations and vibrations of the  $\text{Sm}^{154}$  nucleus is weak and  $K$  is a good quantum number, that between  $\beta$ -motion and  $\gamma$ -motion is not negligible and lowers the phonon states considerably. This coupling between  $\beta$ - and  $\gamma$ -motion comes from quantum mechanical fluctuations which are not negligible even in case of a well-deformed nucleus like  $\text{Sm}^{154}$ . These fluctuations are quite large at an excitation energy of about 2 Mev and lead to tunneling between the prolate shape (the ground state) and the oblate shape of the nucleus. The corresponding states form a metastable band. The  $B(E2)$ 's connecting this band to the ground band are vanishingly small. Therefore, states of this metastable band would decay through the intermediary of either the  $\beta$ -band (the more probable of the two possibilities) or the  $\gamma$ -band, and form a cascade of several  $\gamma$ -rays. The formation of this band would probably be more difficult than its detection. One possible method of formation is the process of double coulomb excitation -- probably a very difficult experiment. However, it would provide a test of the present theory, as well as that of the theory of Coulomb excitation since mixing with the single or direct process would be small.

Calculations involving the application of the present methods to other deformed nuclei, and to spherical nuclei are in progress. A more satisfactory way of determining the parameters of Bohr's Hamiltonian is to calculate them from a microscopic model of the nucleus. Calculations of this type which employ the Pairing-Plus-Quadrupole model are being done<sup>22</sup>.



### Acknowledgements

It is a pleasure to thank W. J. Swiatecki, F. S. Stephens, W. D. Myers, R. M. Diamond, and M. Baranger for stimulating discussions and useful suggestions. The author is grateful to Professor John O. Rasmussen for the excellent facilities of UCLRL, Berkeley, where this work was started during the Summer of 1965, and to Professor Hugh McManus for discussions, support and encouragement. Thanks are also due to the Staff of the Computer Centers of UCLRL and Michigan State University for extensive use of their facilities.

Work performed under the auspices of the United States Atomic Energy Commission.

Present address Krishna Kumar, Department of Physics and Astronomy, Michigan State University, East Lansing, Michigan.

References

1. A. Bohr, Dan. Mat.-Fys.Medd. 26, No. 14 (1952).
2. A. Bohr and B.R. Mottelson, Dan. Mat.-Fys.Medd. 27, No. 16 (1953).
3. E.K. Hyde, I. Perlman and G.T. Seaborg, The Nuclear Properties of the Heavy Elements, Vol. I (Prentice-Hall, 1964), and the references cited there.
4. G. Scharff-Goldhaber and J. Weneser, Phys. Rev. 98, 212 (1955).
5. O. Nathan and S.G. Nilsson in Alpha-, Beta- and Gamma-Ray Spectroscopy, Vol. I, edited by K. Siegbahn (North-Holland, 1965).
6. K. Kumar, Doctoral Dissertation, Carnegie Institute of Technology (December, 1963) unpublished.
7. K. Kumar and M. Baranger, to be published.
8. J.P. Davidson, Rev. Mod. Phys. 37, 105 (1965), and the references cited there.
9. A. Faessler, W. Greiner and R.K. Sheline, Nucl. Phys. 70, 33 (1965).
10. W.D. Myers and W.J. Swiatecki, Nuclear Masses and Deformations, UCRL-11980, to be published.
11. T. Yamazaki, Nucl. Phys. 49, 1 (1963).
12. A.R. Edmonds, Angular Momentum in Quantum Mechanics (Princeton University Press, 1957).
13. A.S. Davydov, Nucl. Phys. 24, 682 (1961).
14. M. Baranger, Phys. Rev. 122, 992 (1961).
15. K. Alder et.al., Rev. Mod. Phys. 28, 432 (1956).
16. L. Wilets and M. Jean, Phys. Rev. 102, 788 (1956).

17. This theorem assumes that the Bohr form of  $T$  or a single  $B$  is used. The degeneracy of the  $2^+$  and  $4^+$  states can be removed by using a different  $B$  for  $\gamma$ -motion<sup>11</sup>. However, Our calculations indicate that this does not give the correct spectrum since the  $3^+$  state, which should move along with this  $2^+$  state, is not affected. Even though the possibility of a different  $B_\gamma$  cannot be ruled out, it probably will not replace a proper  $\gamma$ -dependence of the potential.
18. S.G. Nilsson, Dan. Mat.-Fys. Medd. 29, No. 16 (1955).
19. L. Grodzins, Phys. Letters 2, 88 (1962).
20. Y. Yoshizawa et. al, Nucl. Phys. 73, 273 (1965).
21. A.S. Davydov and G.F. Filippov, Nucl. Phys. 8, 237 (1958).
22. M. Baranger and K. Kumar, to be published.
23. S. Das Gupta and M. R. Gunye, Can.J. Phys. 42, 762 (1964).

## Table Captions

- Table 1. Effects of Dynamics on the Results of  $\text{Sm}^{154}$ . S.M. refers to the static or Rotational model method and D.M. to the present method. In each case, parameters of the collective Hamiltonian are the same as those used for Fig. 1. Methods of calculation are discussed in the text. The excitation energies  $E_I$  are in Mev, the  $B(E2)$  values are in  $e^2 \times 10^{-48} \text{ cm}^4$ , and the spectroscopic quadrupole moments  $Q_I$  are in  $e \times 10^{-24} \text{ cm}^2$ .
- Table 2. Fluctuations and Root Mean Square Values of the Nuclear Shape of  $\text{Sm}^{154}$ . The symbols  $\mathcal{J}, \beta, \gamma, m$  refer to the ground-band,  $\beta$ -band,  $\gamma$ -band, and the metastable-band, respectively. Other quantities have been defined in Section 2.3. Parameters of the Hamiltonian are the same as those used for Fig. 1.
- Table 3.  $B(E2)$  values connecting  $\beta$ -band and  $\gamma$ -band of  $\text{Sm}^{154}$ . Parameters of the Hamiltonian are the same as those used for Fig. 1.

Table 1.

	S.M.	D.M.	EXPT.*
$E_{2+}$	0.072	0.082	0.082
$E_{4+}/E_{2+}$	3.33	3.21	3.26
$E_{0'+}$	1.28	1.09	1.10
$E_{2''+}$	1.80	1.42	1.44
$B(E2; 0 \rightarrow 2)$	4.5	4.7	4.6
$B(E2; 2' \rightarrow 0)$	0.70	0.36	0.47
$B(E2; 2' \rightarrow 2)$			
$B(E2; 2'' \rightarrow 0)$	0.70	0.65	0.65
$B(E2; 2'' \rightarrow 2)$			
$Q_{2+}$	-1.93	-1.97	
$Q_{4+}$	-2.45	-2.54	
$Q_{2'+}$	-1.93	-1.88	
$Q_{4'+}$	-2.45	-2.46	
$Q_{2''+}$	1.93	1.94	
$Q_{3+}$	0.00	0.00	
$Q_{4''+}$	-0.98	-0.97	
$Q_{2'''+}$	-1.93	-0.54	
$Q_{4'''+}$	-2.45	-0.59	

\* Y. Yoshizawa et. al., Nucl. Phys. 73, 273 (1965).

Table 2.

Band	State	$\langle \beta \cos 3\gamma \rangle$	$f_0$	$f_2$	$f$	$\beta_{r.m.s.}$	$\gamma_{r.m.s.}$	$\mu$
g	0+	0.276	0.008	0.037	0.045	0.348	11.14	0.86
	2+	0.281	0.008	0.037	0.045	0.352	11.03	0.85
	4+	0.290	0.007	0.037	0.044	0.358	10.86	0.83
β	0'+	0.248	0.022	0.035	0.057	0.344	11.03	0.98
	2'+	0.266	0.018	0.036	0.054	0.353	10.80	0.93
	4'+	0.281	0.017	0.038	0.055	0.366	10.72	0.91
γ	2''+	0.187	0.018	0.077	0.095	0.361	16.76	1.20
	3+	0.206	0.014	0.079	0.093	0.369	16.57	1.17
	4+	0.214	0.015	0.078	0.093	0.373	16.23	1.16
m	0''+	0.114	0.050	0.037	0.087	0.316	12.48	1.32
	2'''+	0.117	0.052	0.052	0.104	0.342	13.89	1.33
	4'''+	0.98	0.051	0.065	0.116	0.354	15.38	1.36

Table 3.

Transition	B(E2)
0' → 2"	0.019
2' → 2"	0.030
2' → 3	0.011
2' → 4"	0.046
2" → 4"	0.002
3 → 4'	0.044
4' → 4"	0.014

## Figure Captions

Fig. 1. Energy levels and  $B(E2)$  Values for  $\text{Sm}^{154}$ . The lowest  $I=0$  level is labelled  $0+$ , the next one  $0'+$ , and so on. The energy levels have been grouped into the conventional ground-band ( $K=0$ ),  $\beta$ -band ( $K=0$ ),  $\gamma$ -band ( $K=2$ ), and a predicted metastable-band of mixed  $K$ -values. The energies are in Mev and the  $B(E2)$  values are in units of  $e^2 \times 10^{-48} \text{ cm}^4$ . Known experimental data are given in brackets and are taken from Ref. 20. The starred values are uncertain. Comparison with the experimental branching ratios is given in Table 1. The calculated  $B(E2)$  values connecting the  $\beta$ -band and the  $\gamma$ -band are listed in Table 3. Parameters of the collective Hamiltonian are:  $B=127 \text{ (Mev)}^{-1}$ ;  $C=77 \text{ Mev}$ ,  $f=9.7 \text{ Mev}$ ;  $\alpha=0.3$ ,  $G_0=9 \text{ Mev}$ ,  $G_1=-3.5 \text{ Mev}$ , and  $G_2=4.5 \text{ Mev}$ .

Fig. 2. Potential Energy of  $\text{Sm}^{154}$ . This is a polar plot of  $V(\beta, \gamma)$  used for the results of Fig. 1. The lefthand, the righthand, and the uppermost corners of the triangle correspond to  $(\beta=0)$ ,  $(\beta=0.65, \gamma=0^\circ)$ , and  $(\beta=0.65, \gamma=60^\circ)$ , respectively. Equipotential lines are shown. Lowest minimum of this potential occurs at  $\beta=0.33, \gamma=0^\circ$  (prolate), and  $V=5.1 \text{ Mev}$ . There is a second minimum at  $\beta=0.22, \gamma=60^\circ$  (oblate), and  $V=8.0 \text{ Mev}$ . There is a maximum at  $\beta=0$  (spherical) and  $V=9.0 \text{ Mev}$ , and a saddle point at  $\beta \approx 0.24, \gamma \approx 40^\circ$  (non-axial), and  $V=8.6 \text{ Mev}$ .



Fig. 3. Effects of Various Terms of  $V(\beta, \gamma)$  on the Spectrum of  $\text{Sm}^{154}$ . Columns (a), (b), (c), (d), (e), and (f) correspond to the C; C and f; C, f, and  $G_0$ ; C, f,  $G_0$  and  $G_1$ ; C, f,  $G_0$ , and  $G_2$ ; and C, f,  $G_0$ ,  $G_1$ , and  $G_2$  terms of  $V(\beta, \gamma)$  used for Fig. 1.

Fig. 4. Ground State Wavefunction of  $\text{Sm}^{154}$ .  $I=0=K$ . Values of  $A_{\lambda IK}$  are given at each point of the  $\beta$ - $\gamma$  mesh which consists of a large equilateral triangle (with the same dimensions as in Fig. 2.) divided into 256 small triangles. This wavefunction is concentrated in a small region near the lowest minimum of  $V(\beta, \gamma)$  of Figs. 1 and 2. Amplitude of the largest magnitude has been underlined.

Fig. 5.  $\beta$ -band Head Wavefunction of  $\text{Sm}^{154}$ .  $I=0=K$ . Similar to Fig. 4 except that this wavefunction is spread out over a bigger area of the  $\beta$ - $\gamma$  mesh.

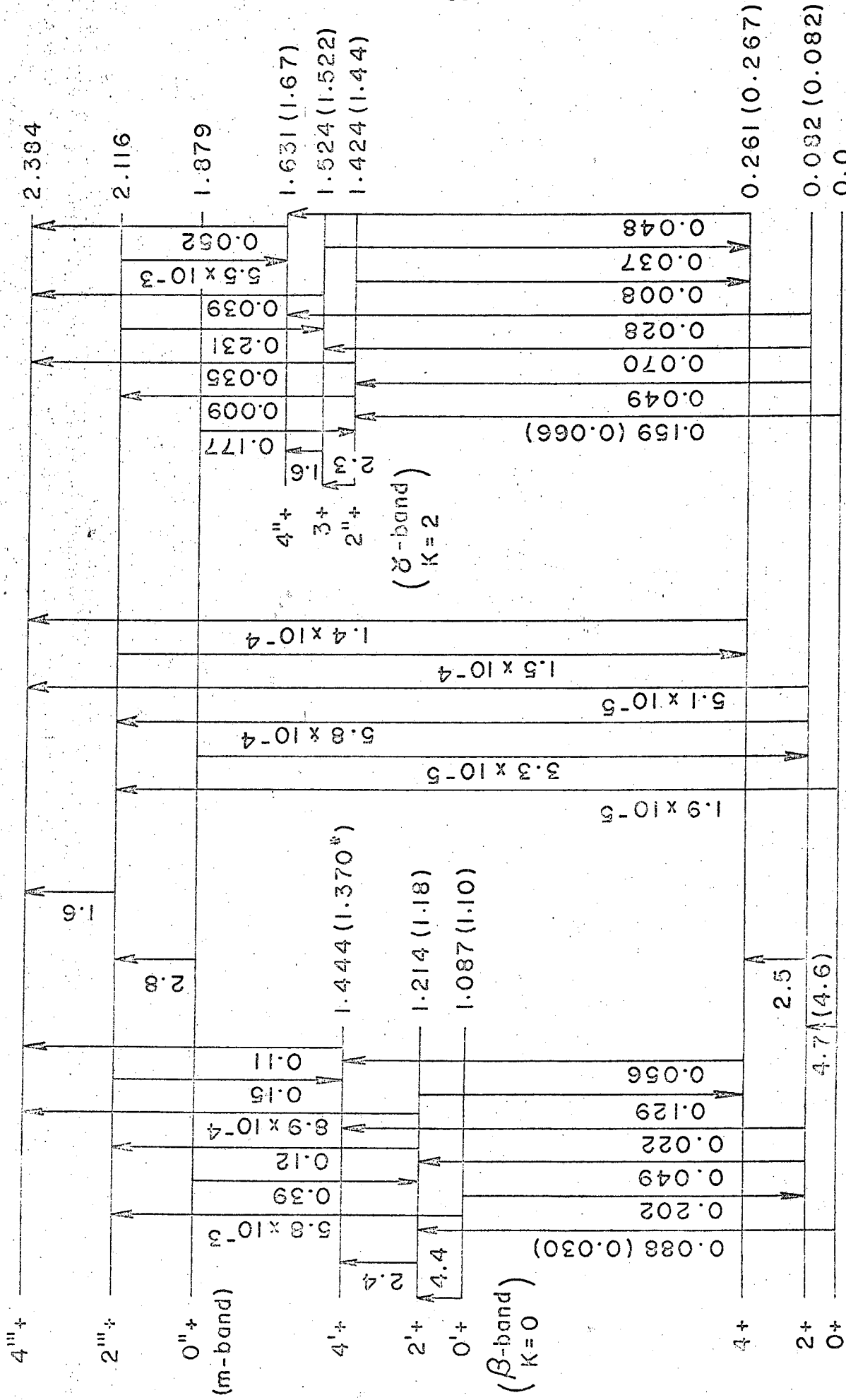
Fig. 6.  $\gamma$ -Band Head Wavefunction of  $\text{Sm}^{154}$ .  $I=2=K$ . This wavefunction vanishes along the  $\gamma=0^\circ$  axis because of symmetry properties of Bohr's Hamiltonian. The  $K=0$  component is practically zero and is not shown.

Fig. 7.  $m$ -Band Head Wavefunction of  $\text{Sm}^{154}$ .  $I=0=K$ . This wavefunction is spread out over practically the whole triangle and has about equal magnitudes for a prolate shape, a spherical shape, and an oblate shape.

Fig. 8. Variation of  $G_0$ .  $G_1=G_2=0$ . Other parameters are the same as those used for Fig. 1.

Fig. 9. Variation of  $G_1$ .  $G_0=10$  Mev (a typical value for a deformed nucleus),  $G_2=0$ . Other parameters as in Fig. 1. Note that the slight asymmetry around  $G_1=0$  is due to the  $f$  term.

Fig. 10. Variation of  $G_2$ .  $G_0=10$  Mev,  $G_1=0$ . Other parameters as in Fig. 1.



154 Sm 92  
62

Fig.1

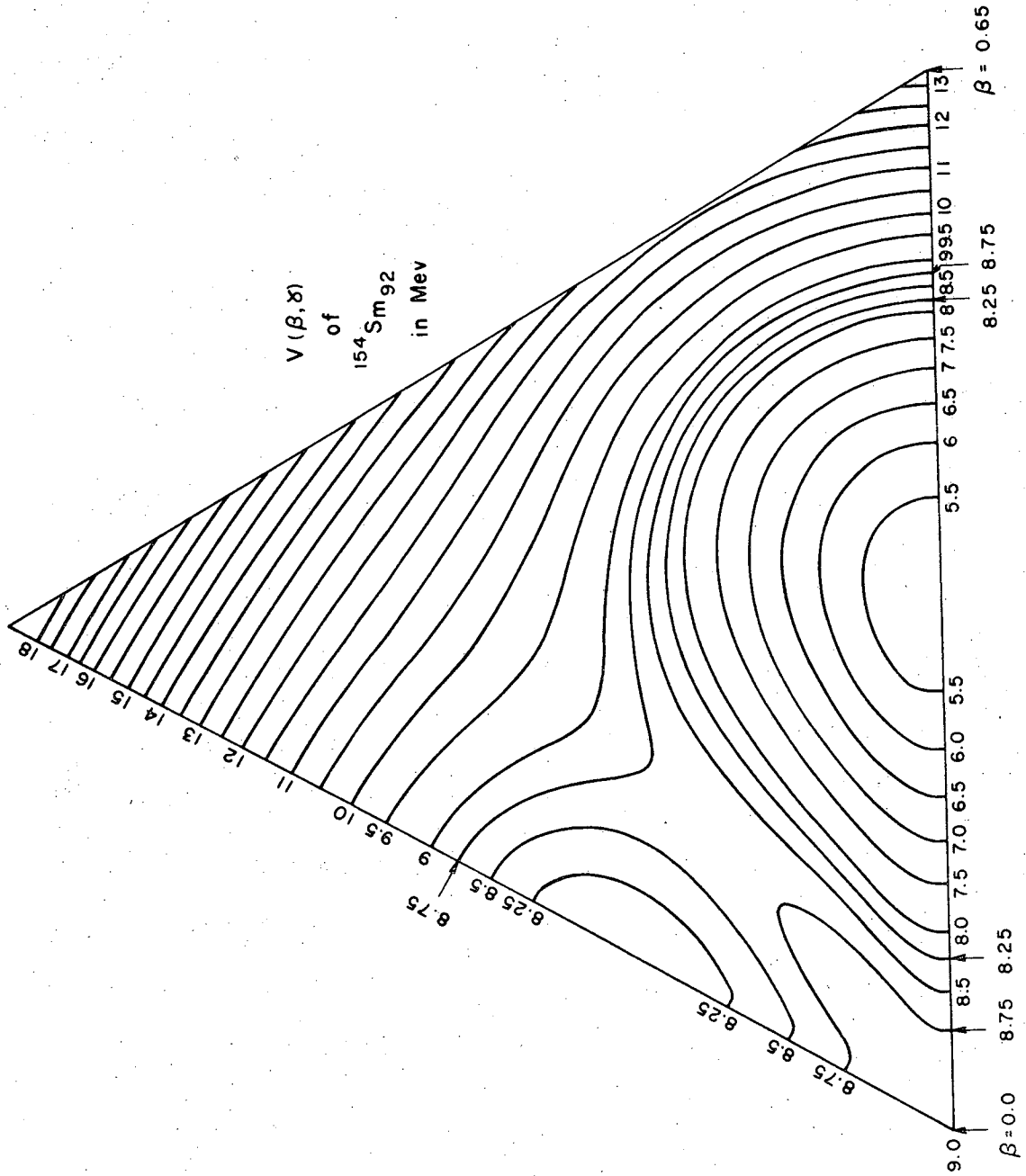


Fig. 2



T= 1 I= 0 K= 0 F.L.A.O.= 1 W.F.A.N.O.= 1

-0.000

-0.000-0.000

-0.000 0.000-0.000

0.000 0.000 0.000 0.000

0.000 0.000 0.000 0.000 0.000

0.000 0.000 0.000 0.000 0.000 0.000

0.000 0.000 0.000 0.000 0.000 0.000 0.000

GR. STATE

0.001 0.001 0.000 0.000 0.000 0.000 0.000 0.000

0.002 0.001 0.001 0.001 0.000 0.000 0.000 0.000

0.005 0.003 0.002 0.002 0.001 0.001 0.001 0.000 0.000

0.009 0.005 0.004 0.004 0.005 0.004 0.004 0.002 0.001 0.000

0.016 0.008 0.008 0.009 0.010 0.011 0.010 0.008 0.005 0.002 0.001 0.001

0.021 0.012 0.011 0.014 0.013 0.023 0.025 0.021 0.015 0.008 0.003 0.001 0.001

0.028 0.016 0.015 0.020 0.030 0.042 0.049 0.048 0.036 0.022 0.010 0.004 0.001 0.001

0.033 0.017 0.020 0.025 0.042 0.063 0.081 0.092 0.072 0.051 0.026 0.011 0.004 0.001 0.001

0.023 0.025 0.020 0.025 0.043 0.071 0.112 0.134 0.131 0.095 0.053 0.023 0.008 0.002 0.001 0.000

0.009 0.021 0.030 0.031 0.031 0.061 0.090 0.119 0.160 0.107 0.085 0.042 0.015 0.007 0.001 0.001 0.000

1 2 3 4 5 6 7 8 9 10 11 12 13 14 15 16 17

Fig. 4

T= 2 1# 0 4# 0 F.L.V.C.S 2 H.F.NO. 2

0.000

-0.000-0.000

-0.000-0.000-0.000

-0.000-0.000-0.000-0.000

-0.000-0.000-0.000-0.000-0.000

-0.000-0.000-0.000-0.000-0.000-0.000

-0.001-0.001-0.000-0.000-0.000-0.000-0.000

154 Sm

-0.000-0.002-0.001-0.000-0.000-0.000-0.000-0.000

P-BAND

-0.007-0.005-0.003-0.001-0.000-0.000-0.000-0.000-0.000

-0.014-0.010-0.007-0.004-0.002-0.000-0.001-0.001-0.001-0.001

-0.023-0.019-0.014-0.009-0.005-0.001-0.002-0.003-0.002-0.002-0.001

-0.028-0.029-0.023-0.020-0.014-0.006-0.002-0.007-0.007-0.005-0.003-0.002

-0.033-0.038-0.038-0.036-0.032-0.019-0.003-0.011-0.017-0.014-0.008-0.004-0.003

-0.021-0.043-0.050-0.053-0.059-0.050-0.022-0.010-0.030-0.032-0.021-0.010-0.004-0.002

0.005-0.036-0.058-0.078-0.098-0.102-0.060-0.011-0.036-0.059-0.043-0.025-0.011-0.004-0.002

-0.313-0.009-0.047-0.081-0.129-0.152-0.145-0.069-0.029-0.082-0.082-0.049-0.021-0.008-0.002-0.001

-0.460-0.017-0.013-0.050-0.105-0.136-0.184-0.086-0.025-0.043-0.105-0.062-0.038-0.018-0.004-0.003-0.001

1 2 3 4 5 6 7 8 9 10 11 12 13 14 15 16 17

Fig. 5

TS 2 IR 2 K=2 F.L.NU. 5 J.F.VO. 7

0.000

0.000 0.000

0.000 0.000 0.000

0.000 0.000 0.000 0.000

0.000 0.000 0.000 0.000 0.000

0.001 0.000 0.000 0.000 0.000

0.002 0.001 0.001 0.001 0.000 0.000

0.005 0.004 0.003 0.002 0.001 0.001 0.000 0.000

0.010 0.008 0.004 0.005 0.003 0.002 0.001 0.001 0.001

0.014 0.013 0.011 0.010 0.008 0.007 0.005 0.003 0.002 0.001

0.020 0.019 0.018 0.016 0.017 0.015 0.012 0.009 0.005 0.002 0.002

0.021 0.023 0.024 0.026 0.028 0.030 0.027 0.021 0.013 0.006 0.003 0.002

0.021 0.023 0.024 0.031 0.040 0.047 0.049 0.042 0.029 0.016 0.007 0.003 0.002

0.020 0.019 0.024 0.031 0.044 0.058 0.069 0.067 0.052 0.032 0.015 0.006 0.002 0.001

0.017 0.014 0.017 0.024 0.037 0.055 0.068 0.078 0.062 0.046 0.024 0.011 0.004 0.001 0.001

0.018 0.010 0.009 0.012 0.021 0.030 0.046 0.051 0.059 0.028 0.012 0.004 0.002 0.000 0.000

0.000 0.000 0.000 0.000 0.000 0.000 0.000 0.000 0.000 0.000 0.000 0.000 0.000 0.000 0.000

1 2 3 4 5 6 7 8 9 10 11 12 13 14 15 16 17

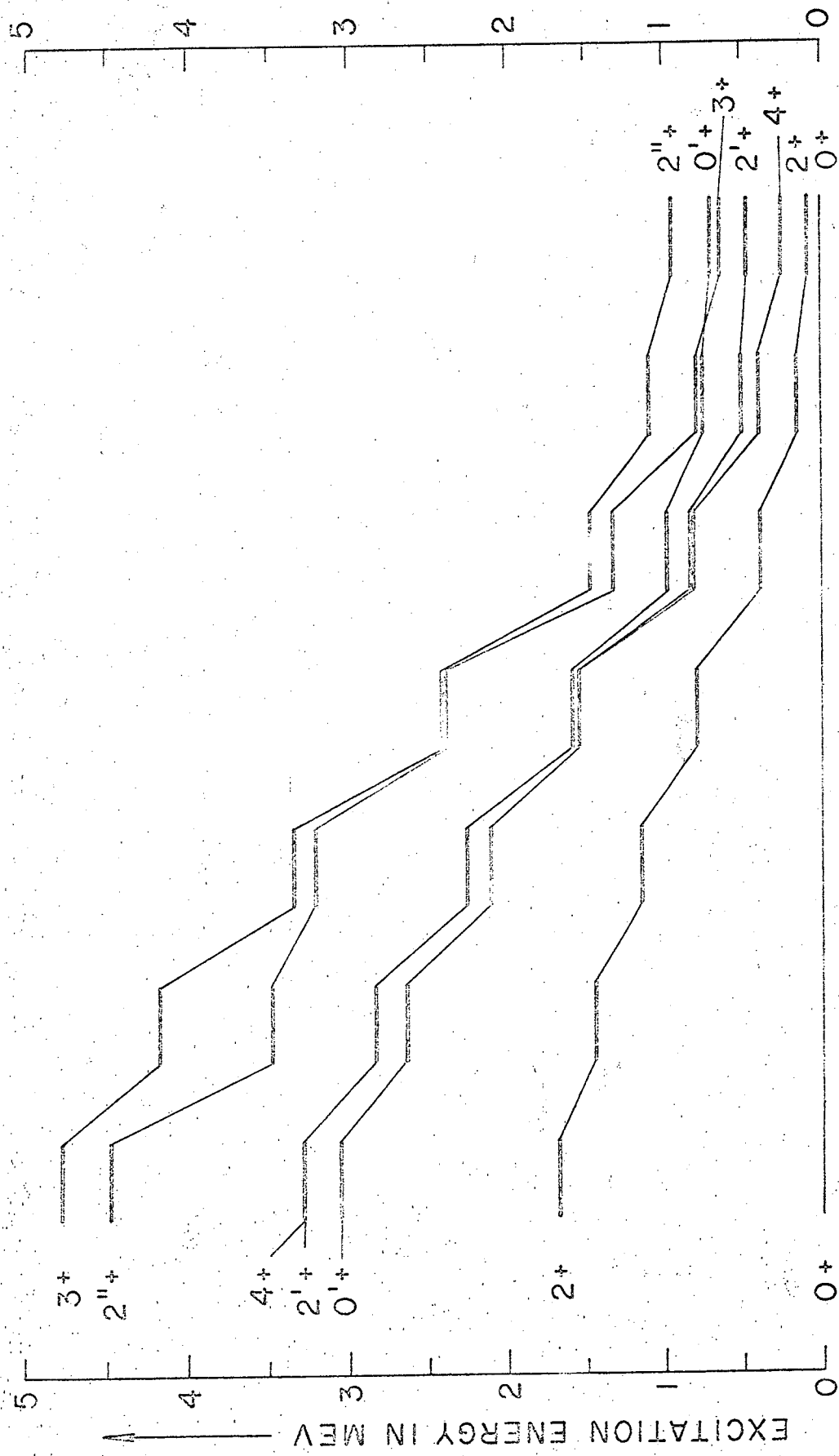
154 Sm

γ-BAND

Fig. 6







$B(E_2; 0 \rightarrow 2)$  0.46 0.53 1.0 2.1 4.1 5.7  
 $G_0$  in Mev -15 -10 -5 0 5 10 15  
—— SPHERICAL ——— DEFORMED ———

Fig. 8



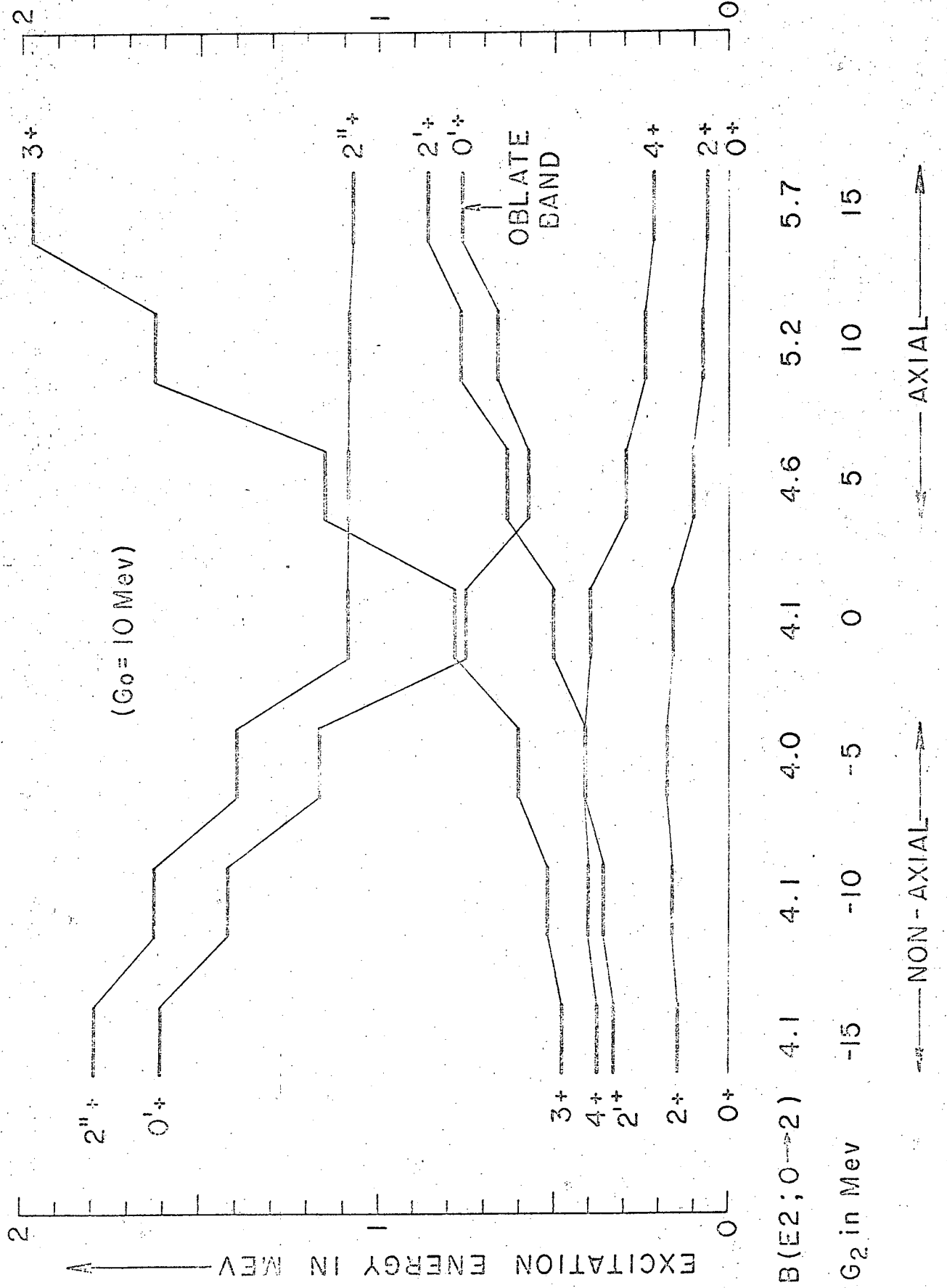


Fig. 10

This report was prepared as an account of Government sponsored work. Neither the United States, nor the Commission, nor any person acting on behalf of the Commission:

- A. Makes any warranty or representation, expressed or implied, with respect to the accuracy, completeness, or usefulness of the information contained in this report, or that the use of any information, apparatus, method, or process disclosed in this report may not infringe privately owned rights; or
- B. Assumes any liabilities with respect to the use of, or for damages resulting from the use of any information, apparatus, method, or process disclosed in this report.

As used in the above, "person acting on behalf of the Commission" includes any employee or contractor of the Commission, or employee of such contractor, to the extent that such employee or contractor of the Commission, or employee of such contractor prepares, disseminates, or provides access to, any information pursuant to his employment or contract with the Commission, or his employment with such contractor.

